RESEARCH SIGNPOST
Research Signpost
37/661 (2), Fort P.O., Trivandrum-695 023, Kerala, India

Recent Developments in Optimization and Optimal Control in Chemical Engineering, 2002. Edited by Rein Luus

Optimal design and operation of an industrial hydrogen plant for multiple objectives

P. P. Oh, Ajay K. Ray and G. P. Rangaiah*
Department of Chemical and Environmental Engineering, National University of Singapore
10 Kent Ridge Crescent, Singapore 119260

Abstract

Many hydrogen plants are currently in operation in chemical and process industries. Increasing demand for hydrogen necessitates optimal additions and changes to these plants. In this work, various retrofitting options for an existing hydrogen plant are considered. For each scenario, optimal design and operating conditions are evaluated to simultaneously maximize hydrogen production and steam generation. First, the heat flux profile in the side-fired reforming furnace is optimized for improved plant performance. Then, two retrofitting cases are considered, namely, debottlenecking waste-heat exchangers and increasing the capacity of the high temperature shift (HTS) and low

Correspondence/Reprint request: G. P. Rangaiah, e-mail: chegpr@nus.edu.sg; fax: (65) 7791936)

temperature shift (LTS) converters. Finally, number and length of tubes in the steam reformer are also optimized. Multi-objective optimization was carried out by a non-dominated sorting genetic algorithm (NSGA). When compared to the work of Rajesh et al. [1] who considered only the optimal operation of the same industrial unit, the present optimization results on retrofitting indicate that significant margin exists for improving existing hydrogen plants.

1. Introduction

Steam reforming is currently the most widely-used process for hydrogen production, accounting for 80% of worldwide production [2]. Demand for hydrogen is growing in many industries, particularly in petroleum refineries in view of heavier and sourer crude, and stricter environmental regulations. It is pertinent, therefore, to consider increasing hydrogen production from existing industrial plants. This can be achieved by operation under optimal conditions and/or by implementing optimized design modifications.

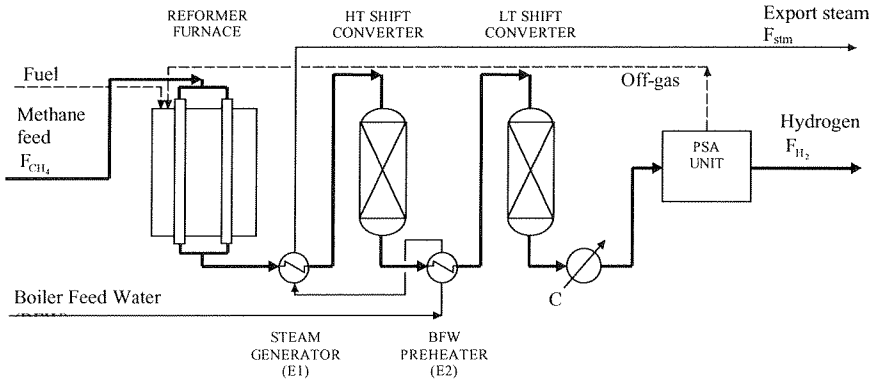

Figure 1. Simplified flowsheet of a typical hydrogen plant

A typical hydrogen plant comprises of two reaction sections – steam reforming and shift conversion. A detailed review of works on reforming and shift conversion kinetics, and on reactor modeling and simulation can be found in Elnashaie and Elshishini [3]. There are also several efforts on the optimization of hydrogen plants. By using a model relating equilibrium reaction kinetics to temperature at every location in the reactor, Davies and Lihou [4] considered the optimal design of a steam reformer. Heat flux profile on the reactor tube was maximized based on an allowable temperature difference across the tube wall toachieve uniform life expectation along the tube length. Thereafter, effect of steam-to-carbon ratio, tube length and wall thickness was studied. The results indicate the existence of an optimum wall thickness giving minimum length for a fixed steam-to-carbon ratio. Glacobbe et al. [5] discussed several revamp options to increase hydrogen production from an existing unit. These include installation of a purge gas booster, addition of LTS reactor, pre-reformer and post-reformer. Depending on the previous design, hydrogen production increase of between 3 and 10% could be achieved. More recently, Rajesh et al. [6] optimized the performance of a side-fired steam reformer for a fixed hydrogen production rate. Dual objectives of minimizing methane feed rate and

maximizing flow rate of carbon monoxide were considered. Subsequently, Rajesh et al. [1] optimized the performance of a hydrogen plant consisting of the steam reformer, shift converters, PSA unit and the associated steam generators, for simultaneous maximization of hydrogen product and export steam flow rates for a fixed methane flow rate. Design limitations (i.e., without retrofitting existing equipment) were taken into consideration in both studies and improvement was sought by optimization of operating variables alone.

In this work, optimal retrofitting of an existing hydrogen plant along with operating variables, for maximizing both hydrogen and export steam produced is studied. The model of the hydrogen plant developed by Rajesh et al. [1] is adapted for this purpose. Performance enhancement is first sought by optimizing heat flux profile in the steam reformer. Then, installation of larger waste-heat exchangers followed by increasing the capacity of the shift converters are considered. Finally, number and length of tubes in the reformer are also optimized. These modifications do not require major structural changes. An adaptation of the genetic algorithm (GA) is used for solving the resulting two-objective optimization problems. Performance of the various retrofitting cases is compared with the results of Rajesh et al. [1] for optimal operation of the existing plant.

2. Optimization techniques

Many methods are available for solving optimization problems with single objective function [7, 8]. Some of these are direct search methods using only the values of objective function. Others which employ both the objective function value and its derivatives, are the indirect or gradient search methods. These latter methods are generally more efficient. All these methods are, however, only capable of finding only a local minimum. In recent years, methods for global optimization are receiving increasing attention [7]. These include stochastic methods such as GA, simulated annealing, taboo search, which can often locate the global optimum.

In contrast to the plethora of techniques available for single-objective optimization, relatively few techniques have been developed for solving optimization problems with two or more objectives. Examples include weighted sum strategy, epsilon-constraint method and goal attainment method which simplify the optimization problem by either combining multiple objectives into one with suitable weights or focusing on one objective at a time. Adaptations of GA, can handle multiple objectives simultaneously without simplification, are also available [8]. One such adaptation – non-dominated sorting Genetic Algorithm (NSGA) was used in this work. The principle and algorithm of NSGA are presented in Appendix I. More details on NSGA are available elsewhere [9-11].

3. Process Description

A simplified flow sheet of the hydrogen plant is shown in Fig. 1. Other designs may vary from this in terms of the presence of a pre-reformer, design of the reformer furnace (side-fired or top-fired) and the extent of heat integration. Natural gas (assumed to consist of methane as the only hydrocarbon) is mixed with appropriate quantities of steam and recycle hydrogen. The mixed stream then enters the tubes in the steam

reforming furnace. The following important reactions occur at high temperatures over nickel-based catalyst in the reformer tubes:

$$CH_4 + H_2O \leftrightarrows CO + 3H_2$$
$$-(\Delta H_r) = 2.06\times10^5 \text{ kcal/kmol} \quad (1)$$
$$CO + H_2O \leftrightarrows CO_2 + H_2$$
$$-(\Delta H_r) = -4.11\times10^4 \text{ kcal/kmol} \quad (2)$$
$$CH_4 + 2H_2O \leftrightarrows CO_2 + 4H_2$$
$$-(\Delta H_r) = 1.65\times10^5 \text{ kcal/kmol} \quad (3)$$

The sensible heat of the reformer effluent is recovered in a waste-heat exchanger (E1) to generate high pressure steam for internal use and for export outside the unit. Carbon monoxide is converted via shift reaction (Eq. (2)) in a HTS reactor and subsequently in a LTS reactor, after which hydrogen is recovered and purified in a pressure-swing adsorption (PSA) unit. Heat is recovered from the HTS reactor effluent in a second waste-heat exchanger (E2) and used to preheat boiler feed water (BFW). Finally, off-gases from the PSA unit are used to supplement natural gas fuel for combustion in the reforming furnace.

4. Modeling & Simulation

A rigorous model of the hydrogen plant developed by Rajesh et al. [1, 6] was adapted for use in this work. In their work, the reaction model of Xu and Froment [12] was used without modification. A simplified version of the dusty gas model recommended by Elnashaie and Elshishini [3] was adopted. The method of orthogonal collocation on finite elements (OCFE) [13] was employed to obtain the intra-pellet concentration profiles and then effectiveness factors at any axial location in the reformer tube. The HTS and LTS converter models are similar to that of Elnashaie and Alhabdan [14]. The PSA unit was simulated as a 'black box' with 90% recovery and 99.95% purity in the hydrogen product. More details on the model of the hydrogen plant are available in Rajesh et al. [1, 6]

While adapting and testing the programs of Rajesh et al. [1] for this work, a programming error in the steam generation part was uncovered. The error allowed good amounts of steam generation in waste-heat exchangers, E1 and E2. Upon correction, little or no steam, in excess of internal use, was available for export. This in turn led to a shortcoming of the model of Rajesh et al. [1], namely, failure to account for steam generation by heat recovery from the flue gas exiting the steam reformer in the convection section of the furnace. In typical industrial hydrogen plants, this source accounts for approximately 60% of total steam generation with the balance from energy recovery in E1 and E2. In this work, an energy balance was performed to estimate the heat duty of exchangers (E1 and E2 in Fig. 1) and then calculate the quantity of steam produced iteratively. Assuming that this amount accounts for 40% of total steam generation, total and export steam generation were estimated.

The model described above was modified to use the heat flux profile as a decision variable. This required adapting heat transfer equations of Singh and Saraf [15] to solve for the tube wall and process gas temperatures using the heat flux at any axial location. The model was simulated on the SGI Origin 2000 supercomputer using the mathematical routines, DIVPAG (for integration of stiff ordinary differential equations) and DNEQNF (for solving the set of non-linear collocation equations) of IMSL.

5. Formulation of the optimization problem

For a fixed feed rate of methane, the economics of a hydrogen plant are governed primarily by the income from product hydrogen and export steam (steam production in excess of internal use). For want of generalized cost data and to obtain a wide range of optimal results, product hydrogen and export steam flow rates can be maximized simultaneously. The optimization problem is:

Maximize:

$$J_1 = F_{H_2} \quad (4)$$

$$J_2 = F_{stm} \quad (5)$$

subject to:

$$T_{w,max} \leq 1200 \text{ K} \quad (6)$$

$$\left[\frac{y_{H_2O}}{y_{H_2}}\right]_{HTS} \geq 0.3 \quad (7)$$

$$T_{LTS} \geq (T_{dew} + 15) \text{ K} \quad (8)$$

$$F \leq 1.2\, F_{max} \quad (9)$$

$$Q_{Ei} \leq 1.2\, Q_{Ei\,max} \quad i = 1, 2 \quad (10)$$

Eq. (6) is based on the creep limit of alloy steel tubes at operating conditions and is required to prolong tube life. The constraint in Eq. (7) is to avoid methanation reaction in the shift converter. Process gas temperature in the LTS is maintained at least 15^0C above its dew point (Eq. (8)) to prevent steam condensation in the catalyst pores, leading to deactivation. Equations (9) and (10) ensure that plant operation is within design margins.

Rajesh et al. [1] solved the optimization problem described above for an existing hydrogen plant. They obtained sets of optimal values only for the operating variables, namely, $T_{SMR,in}$, $P_{SMR,in}$, $(H/C)_{in}$, $(S/C)_{in}$, T_g, $T_{HTS,in}$ and $T_{LTS,in}$, for the best possible unit performance. The bounds on these decision variables, with the exception of T_g, are the same as those listed later in Eqs. (12a) to (12d), (12k) and (12l). Bounds on T_g, 1375 and 1675 K, are both based on normal operating ranges in industrial units. The set of optimal solutions they obtained is corrected for the error in the steam generation part and used as the basis for comparing the performance of the various retrofitting scenarios studied in this work. The four options considered for improvement are additive. Hence, the number of decision variables and required capital investment increase from Case 1 to Case 4.

Case 1: Optimal Heat Flux Profile In Steam Reformer

In comparison to top-fired furnace designs, the side-fired design is characterized by the presence of many burners at different heights. This allows for easy adjustment of heat input to each burner and consequently the heat flux profile on reformer tubes. Hence, performance improvement of the hydrogen plant is first sought by operating the steam reformer under an optimal heat flux profile.

The axial heat flux profile for a side-fired reformer typically peaks near the entrance of the tube [16]. This profile is best modelled with two quadratic functions which define two sections of the reformer tube preceding and following z^* where heat flux is maximum. In addition, these functions are equal at z^* to ensure that they describe a continuous profile.

For $z \leq z^*$,

$$q = A + B(\frac{z}{z^*}) + C(\frac{z}{z^*})^2 \quad (11a)$$

For $z > z^*$,

$$q = A + B + C + D(\frac{z - z^*}{L_{SMR}}) + E(\frac{z - z^*}{L_{SMR}})^2 \quad (11b)$$

where z is any axial point along the tube and L_{SMR} is the total tube length. The coefficients A to E and z^* in the above equations specify the heat flux profile.

The optimization problem in this case is solved with twelve decision variables, six of which are identical to those used by Rajesh et al. [1] and the remaining variables are A to E and z^*. Bounds on these variables are

$725 \leq T_{SMR,in} \leq 900$ K (12a)
$2450 \leq P_{SMR,in} \leq 2950$ kPa (12b)
$2.0 \leq (S/C)_{in} \leq 6.0$ (12c)
$0.0 \leq (H/C)_{in} \leq 0.5$ (12d)
$20 \leq A \leq 80$ Mcal m^{-2} h^{-1} (12e)
$0 \leq B \leq 60$ Mcal m^{-2} h^{-1} (12f)
$-30 \leq C \leq 0$ Mcal m^{-2} h^{-1} (12g)
$-60 \leq D \leq 0$ Mcal m^{-2} h^{-1} (12h)
$-60 \leq E \leq 30$ Mcal m^{-2} h^{-1} (12i)
$0.5 \leq z^* \leq 2.0$ m (12j)
$570 \leq T_{HTS,in} \leq 730$ K (12k)
$400 \leq T_{LTS,in} \leq 530$ K (12l)

The lower limit on $T_{SMR,in}$ is to prevent gum formation in the catalyst, while its upper limit is based on the maximum heat typically transferred from flue gas to the feed mixture in the convection section of the reforming furnace. The lower and upper bounds on $P_{SMR,in}$ are based on the pressure required of product hydrogen and on the supply pressure of the feed respectively. Bounds on $(S/C)_{in}$ are chosen based on the normal operating range in industrial units. A very low value of $(S/C)_{in}$ may cause coking, shift-reaction problems, and even high methane leakage from the reformer. Higher $(S/C)_{in}$ increase mass flow through the plant, and thus the size and cost of the equipment. Upper limit on $(H/C)_{in}$ is selected to avoid redundant hydrogen recycle back to the reformer. Bounds on $T_{HTS,in}$ and $T_{LTS,in}$ are based on normal operating ranges in industrial units. Reliability of reformer tubes is of concern to avoid down-time due to tube failure. The possibility of creep damage from thermal-gradient stress across the tube wall limits the maximum heat flux that can be safely applied, which typically varies from 95 to 110 Mcal m^{-2} h^{-1} [17]. Conservative limits for q between 20 and 80 Mcal m^{-2} h^{-1} are chosen. Bounds for A correspond to the limits on q, while those for B to E allow maximum flexibility in describing the profile while ensuring zero slope at the maximum point, $z = z^*$. Typical limits for z^* are chosen [16].

Case 2: De-Bottlenecking Waste Heat Exchangers

For the hydrogen plant under consideration, heat recovered in the reformer and HTS effluent waste-heat exchangers (E1 and E2 in Fig. 1) serves to raise steam from

boiler feed water (BFW). The possibility of increased steam generation by de-bottlenecking these exchangers (presently constrained by design margins according to Eq. (10)) is studied by performing optimization without the constraints on heat exchanger capacities (These constraints, Eq. (10) were also not included in the subsequent cases.). This may require debottlenecking the steam generators in the convection section of the reformer furnace since total steam generated in the plant for the present study is assumed to be proportional to steam generated in E1 and E2 (Fig. 1).

Case 3: Optimal Design Of Shift Converters

A shift converter, besides increasing hydrogen yield and steam production, minimizes the amount of CO in the feed to the PSA, thereby improving the efficiency and capacity of the PSA unit. The potential of optimizing shift converters to increase these benefits is considered in this case. To minimize capital investment, HTS and LTS reactors in a hydrogen plant are usually identical. Hence, for optimization purposes, these two reactors are assumed to be of identical size. The two additional decision variables are length and diameter of the catalyst beds (L_{shift} and D_{shift}). The following limits and constraint are placed on these two variables which are optimized along with the decision variables in Eqs. (12a) to (12l).

$$2.0 \leq D_{shift} \leq 4.0 \text{ m} \qquad (13a)$$

$$2.0 \leq L_{shift} \leq 5.6 \text{ m} \qquad (13b)$$

$$1.0 \leq L_{shift}/D_{shift} \leq 1.4 \qquad (13c)$$

The upper bound on D_{shift} is determined based on the desired Reynolds number, Re, in the reactor. Both the heat and mass transfer coefficients in the catalyst bed are based on empirical j-factor correlations, which are functions of Re. For a fixed methane feed rate to the hydrogen plant, the flow entering the HTS converter can be estimated by assuming a typical methane conversion in the reformer. Typical values are also assumed for average molecular weight and viscosity of the process gas. In this way, Re is governed by the cross-sectional area of the catalyst bed and hence dependant solely on D_{shift}. As the j-factor correlations used in the model are valid only for Re > 350 [14], the lower bound on D_{shift} ensures that Re does not fall below this limit. The chosen limit for Re is also consistent with the operation in industrial shift reactors [14] where Re varies from 400 to 1000. The limits on L_{shift} and on the aspect ratio (Eqs. (13b) and (13c)) are also selected based on typical HTS and LTS reactor catalyst bed dimensions [14, 18, 19].

Case 4: Optimal Design Of Steam Reforming Furnace

Productive modifications of the furnace are impossible without a complete overhaul of the existing design [20]. Important parameters in reforming furnace design include volume of the furnace, number, thickness and arrangement of tubes, and arrangement of burners. Volume of the furnace is dependant on tube pitch, number of tube passes, number and size of tubes. The tubes may be arranged in parallel, staggered or straight rows. Tube pitch affects the physical size and, thereby, furnace cost. In addition, it dictates the extent of shielding between tubes, affecting heat transfer to individual tubes and, consequently, tube life [20]. The model used in this work regards the performance of a single reformer tube to be representative of all others. This implies that the effect of tube pitch and number of tube passes on radiative heat transfer from the furnace gas to tubes is not considered. Therefore, these parameters cannot be included as

variables for optimization and are left to the discretion of the designer, who will select an appropriate and economical arrangement.

The minimum tube diameter is based on the smallest ratio between tube and catalyst pellet diameters. In general, it is economical to use the largest possible diameter while taking process severity and economic tube wall thickness into consideration [4]. For a given tube diameter, wall thickness is determined based on design pressure and allowable stress on the tube. The latter is dependant on the desired tube life in relation to the wall temperature and material of construction [16]. It is desirable to minimize wall thickness as a thinner wall implies lower resistance to heat transfer, resulting in lower tube wall temperature and longer tube life [20]. Tube inner diameters ranging from 70 to 160 mm with a wall thickness between 10 and 20 mm are used in practice [16]. In view of the many factors involved in determination of tube diameter and wall thickness, some of which are not represented in the model, these parameters are considered fixed in this study. Tube inner diameter of 79.5 mm with wall thickness 22.5 mm are adopted from the hydrogen plant modelled [3].

Two furnace design variables, namely, the number and length of tubes, were considered in Case 4 for optimizing steam reformer in addition to all the modifications in Cases 1 to 3. Between 40 and 400 tubes are typically used in a reformer, with heated length from 6 to 12 m depending on furnace type [16]. The lower bound for number of tubes (N_{tub}) was increased to 120 based on the throughput in the unit in order to ensure Reynolds number in the order of 10,000 in the steam reformer according to industrial practice [16]. The bounds used for the decision variables are thus:

$$120 \leq N_{tub} \leq 400 \qquad (14a)$$

$$6.0 \leq L_{SMR} \leq 12.0 \text{ m} \qquad (14b)$$

These decision variables are used along with those from Case 3 (Eqs. (12a) to (12l) and (13a) to (13c)). Reformers are typically operated at high pressures to allow a reduction in the size of process equipment and to minimize the cost of compressing product hydrogen. An additional constraint on the maximum pressure drop is thus required.

$$\Delta P_{SMR} \leq 400 \text{ kPa} \qquad (15)$$

This constraint is added to those from Eqs. (6) to (8) in the optimization problem.

Optimization Problem

Since the optimization program is for minimization, maximization of F_{H_2} and F_{stm} is reformulated as minimization of their reciprocals. The performance constraints (Eqs. (6) to (10) and (15)) were also incorporated into the objective functions as penalty functions. The optimization problems can now be written as:

Minimize:

$$I_1 = \frac{1}{F_{H_2}} + 10^4 \sum_{i=1}^{n} f_i \qquad (16)$$

$$I_2 = \frac{1}{F_{stm}} + 10^4 \sum_{i=1}^{n} f_i \qquad (17)$$

where

$f_1 = (T_{w,max}-1200)+|(T_{w,max}-1200)|$ (18a)

$$f_2 = [0.3 - \frac{y_{H_2O}}{y_{H_2}}] + |[0.3 - \frac{y_{H_2O}}{y_{H_2}}]| \quad (18b)$$

$f_3 = ((T_{dew}+15)-T_{LTS})+|(T_{dew}+15)-T_{LTS}|$ (18c)

$f_4 = (F-1.2F_{max})+|(F-1.2F_{max})|$ (18d)

$f_5 = (Q_{E1}-1.2Q_{E1\,max})+|(Q_{E1}-1.2Q_{E1\,max})|$ (18e)

$f_6 = (Q_{E2}-1.2Q_{E2\,max})+|(Q_{E2}-1.2Q_{E2\,max})|$ (18f)

$f_7 = (\Delta P_{SMR}-400)+|(\Delta P_{SMR}-400)|$ (18g)

Note that n = 1 to 6 for Case 1, n = 1 to 4 for Cases 2 and 3, and n = 1 to 3 and 7 for Case 4.

In Eqs. (16) and (17), the large weighting factor on constraints penalizes the objectives in the event of constraint violation. It was found that the value of the weighting factor is not important (as long as it is reasonably large). This is due to a marginal effect of nonlinearities and discontinuities on GA. The optimization problem for each case was solved using NSGA. Values of its parameters are: number of chromosomes (or population size) = 50, length of chromosomes = 32 bits, crossover probability = 0.70, mutation probability = 0.002, spreading parameters, α = 2.0 and σ = 0.05, and the number of generations = 150.

6. Results And Discussion

An inherent conflict is present between two objective functions involved in multiobjective optimization when they are influenced in opposite directions by changes in some decision variables. As a result, multiple optimal solutions (forming a Pareto set) will be encountered. Each of these Pareto-optimal solutions (or chromosomes in GA context) is superior to another in terms of one or more objectives, but inferior in terms of others. Hence the selection of the 'best' solution among them will be based on (usually non-quantifiable) criteria that were not included in the optimization.

While performing optimization, many chromosomes were penalized for violating the restrictions on heat flux, q. This adversely affects the efficiency of optimization and is attributed to the wide ranges for variables B to E (Eqs. (12f) to (12i)). These, variables were limited based on values selected for the preceding variables (see Eqs. (19a) to (19d) below) to ensure that the heat flux always fell within acceptable bounds. The lower limit for C and upper limit for E were also dependant on the values of B and D respectively, to ensure that the profile saturates appropriately at the maximum point. The redefined bounds are:

$0 \le B \le (80 - A)$ (19a)

$-0.5B \le C \le 0$ (19b)

$(20-A-B-C) \le D \le 0$ (19c)

$(20-A-B-C-D) \le E \le -0.5D$ (19d)

The mapping of these variables from binary to decimal system in NSGA was done using these bounds in place of those in Eqs. (12f) to (12i). Similarly, the mapping of D_{shift} was performed based on L_{shift} using the limits of Eq. (13c) instead of those in Eq. (13a).

The Pareto optimal solutions obtained from each of the four retrofitting cases of the existing design configuration are shown in Fig. 2. For Case 1, all decision variables are

plotted against F_{H_2} in Fig. 3, while for other cases only those variables that contribute to the conflict in the objective functions, namely, $(S/C)_{in}$ and $(H/C)_{in}$, are shown (Fig. 4). The heat flux profile representative of the respective Pareto sets are shown in Fig. 5. The operating parameters of two chromosomes from the Pareto set are shown in Table 1. All these results are discussed below.

Case 1: Optimal Heat Flux Profile In Steam Reformer

The decision variables associated with the chromosomes of the Pareto set of Case 1 in Fig. 2, are shown in Fig. 3. The reactor inlet temperatures, $T_{SMR,in}$, $T_{HTS,in}$ and $T_{LTS,in}$ (Fig. 3a) are practically constant. The endothermic reforming reactions (Eqs. (1) and (3)), and the exothermic shift conversion reactions (Eq. (2)) are favoured at high and low temperatures, respectively. The optimized solutions thus predict operation at the upper limit of $T_{SMR,in}$ (Fig. 3a). Contrary to expectation, the optimal $T_{HTS,in}$ and $T_{LTS,in}$ (Fig. 3a) do not fall near their lower bounds. These values, are, however, the lowest possible with respect to the maximum cooling duty that can be extracted from the heat exchangers at the reformer and HTS reactor exits. Hence, given the design constraints (Eq. 10), these operating conditions allow the highest possible methane conversion in the reformer and shift converters, leading to increased hydrogen production.

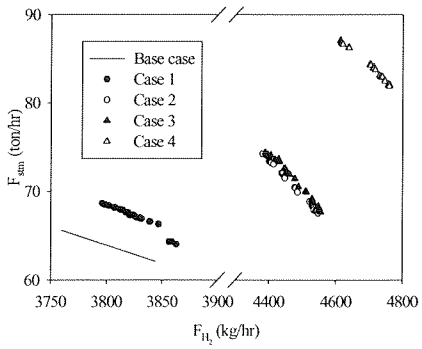

Figure 2. Pareto-optimal sets for various cases as compared with the base case for which T_g, instead of heat flux profile, is used as a decision variable.

Lower pressure enhances the reforming reactions (Eqs. (1) and (3)) leading to higher hydrogen production (Fig. 3b), while the shift reaction (Eq. (2)) is unaffected by pressure. The effect of pressure on steam generation is more indirect. Steam is raised from BFW through heat recovery from the reformer and HTS reactor effluents. Lower pressure increases the extent of the forward reforming reactions in the reformer, thereby necessitating greater heat of reaction. This implies that for a fixed heat input to the reformer, less heat will be available for recovery and steam generation in E1. On the other hand, lower pressure results in the first reforming reaction (Eq. (1)) dominating over the second (Eq. (3)), producing relatively more CO and less CO_2. This increases the extent of exothermic shift conversion in the HTS reactor and the amount of heat available to preheat BFW in E2. Thus, lower pressure decreases heat recovery in E1 while increasing the same in E2. Consequently, the overall effect of pressure on steam generation depends on the operating conditions. This has been confirmed by sensitivity analysis performed at conditions corresponding to a few chromosomes. Hence, optimal values of $P_{SMR,in}$ are scattered although they are all near the lower limit (Fig. 3b) where more hydrogen can be produced.

Fig. 3c shows that optimal $(S/C)_{in}$ increases from 4.0 to 4.2 with hydrogen production. An increase in $(S/C)_{in}$ promotes the reforming reactions, thus increasing methane conversion and hydrogen production (Fig. 3c). However, increase in $(S/C)_{in}$ also favours the second reforming reaction (Eq. (3)) over the first (Eq. (1)), generating relatively more CO_2, and less CO, in the reformer outlet. This in turn decreases conversion in the shift converters and available heat for recovery in E2 for BFW preheating and thereby steam generation. An increase in $(H/C)_{in}$ inhibits the reforming reactions, thus reducing hydrogen production (Fig. 3d). At the same time, it inhibits the second reforming reaction (Eq. (3)) more than the first (Eq. (1)), generating more CO in the reformer outlet for increased reaction in the shift converters and consequently increased steam generation. Hence both $(S/C)_{in}$ and $(H/C)_{in}$ have conflicting effects on F_{H_2} and F_{stm}.

As can be seen from the optimal values of two chromosomes G and H for Case 1 in Table 1, all chromosomes have very similar optimal values for the variables A, B, D, E and z^*, which define the heat flux profile according to Eq. (11). Although C value is different, it has negligible effect on the heat flux profile. This implies that the entire Pareto set of solutions have nearly identical optimal heat flux profiles. A typical optimal profile is shown in Fig. 5. The heat flux is near its upper limit in the first meter of the reformer, before falling to a low value. This is consistent with the heat required for reactions occurring in the tubes. It should be possible to achieve the optimal heat flux profile by adjusting the firing of burners in the side-fired reformer.

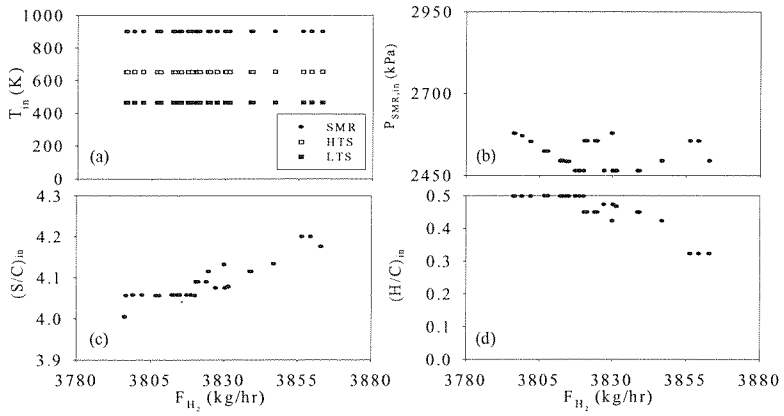

Figure 3. Decision variables associated with the Pareto set of Case 1 shown in Fig. 2

Comparison of the results of Case 1 with the base case obtained by optimization with T_g as a decision variable (which are the corrected results of Rajesh et al. [1]) reveals that operating the reformer furnace under an optimal heat flux profile leads to approximately 2% and 10% increase in hydrogen production and steam generation, respectively (Fig. 2). A heat flux profile representative of the chromosomes in the case with T_g as the decision variable (Fig. 5), is relatively constant throughout the tube length, varying between 55 and 70 Mcal m^{-2} h^{-1}. The optimized profile supplies approximately 15% more heat in the initial 5 m of the tube to fire the bulk of reactions taking place in

that section, thus accounting for the improvement in objectives. On the whole, operating with an optimal heat flux requires about 5% increase in the reformer heat duty, which is supplied by PSA off-gas supplemented by additional furnace fuel. As the cost of additional fuel affects the profitability of the hydrogen plant, this factor has to be taken into account when evaluating the economics of such an operation.

Table 1 Operating parameters for selected chromosomes of the Pareto-optimal sets in Fig. 2

Parameter	Values corresponding to selected chromosomes							
	Case 1		Case 2		Case 3		Case 4	
	G	H	I	J	K	L	M	N
Operating variables								
$T_{SMR,in}$	900.0	900.0	899.0	899.0	899.2	899.2	790.6	790.6
$P_{SMR,in}$	2577.9	2493.8	2495.8	2460.7	2463.5	2459.6	2473.4	2457.8
$(H/C)_{in}$	0.497	0.422	0.468	0.032	0.390	0.023	0.397	0.152
$(S/C)_{in}$	4.00	4.13	5.42	5.45	5.53	5.54	5.47	5.60
$T_{HTS,\ in}$	654.5	654.5	629.5	629.4	601.7	591.3	598.3	598.6
$T_{LTS,in}$	467.1	467.2	465.2	465.2	466.1	466.3	465.7	465.7
A	74.4	74.3	79.8	79.8	80.0	80.0	78.0	79.5
B	2.81	2.81	0.213	0.206	0.035	0.029	1.20	0.483
C	-0.0075	- 0.0005	- 0.0068	-0.010	- 0.0007	- 0.0006	-0.143	- 0.0345
D	-35.7	-35.7	-3.87	-3.78	-3.99	-3.99	-15.6	-15.5
E	7.93	8.00	-19.9	-20.0	-20.2	-20.2	-41.7	-41.9
z^*	1.25	1.25	1.99	1.99	2.00	2.00	1.98	1.98
F_{H_2}	3796	3847	4381	4548	4430	4553	4638	4739
F_{stm}	68.6	66.3	74.2	67.5	74.4	67.7	86.3	82.9
Q_{SMR}	108.9	108.9	125.9	126.2	126.1	126.0	150.5	151.0
Q_{E1}	18.7	9.7	24.2	23.1	25.5	25.1	28.0	27.7
Q_{E2}	9.6	9.8	10.4	10.1	9.3	8.5	9.5	9.4
Design variables								
L_{shift}	**4.40**	**4.40**	**4.40**	**4.40**	5.54	5.54	4.90	4.90
D_{shift}	**3.12**	**3.12**	**3.12**	**3.12**	3.98	4.00	3.94	3.94
N_{tub}	**176**	**176**	**176**	**176**	**176**	**176**	237	237
L_{SMR}	**11.95**	**11.95**	**11.95**	**11.95**	**11.95**	**11.95**	12.00	12.00

Note: Design variables in bold print are for the existing plant configuration and have not been optimized in these cases.

Case 2: De-Bottlenecking Waste Heat Exchangers

The Pareto-optimal set obtained for this case is shown in Fig. 2. Increasing the capacity of the waste-heat exchangers, Q_{E1} and Q_{E2}, lead to nearly 20% improvement in hydrogen production and nearly 10% improvement in steam production. Table 1 shows the decision variables associated with two selected chromosomes of the Pareto set for Case 2. Similar to Case 1 (Fig. 3), optimized values of $T_{SMR,in}$ fall near its upper bound while those of $P_{SMR,in}$ are scattered nearer its lower bound. In addition, narrow range of

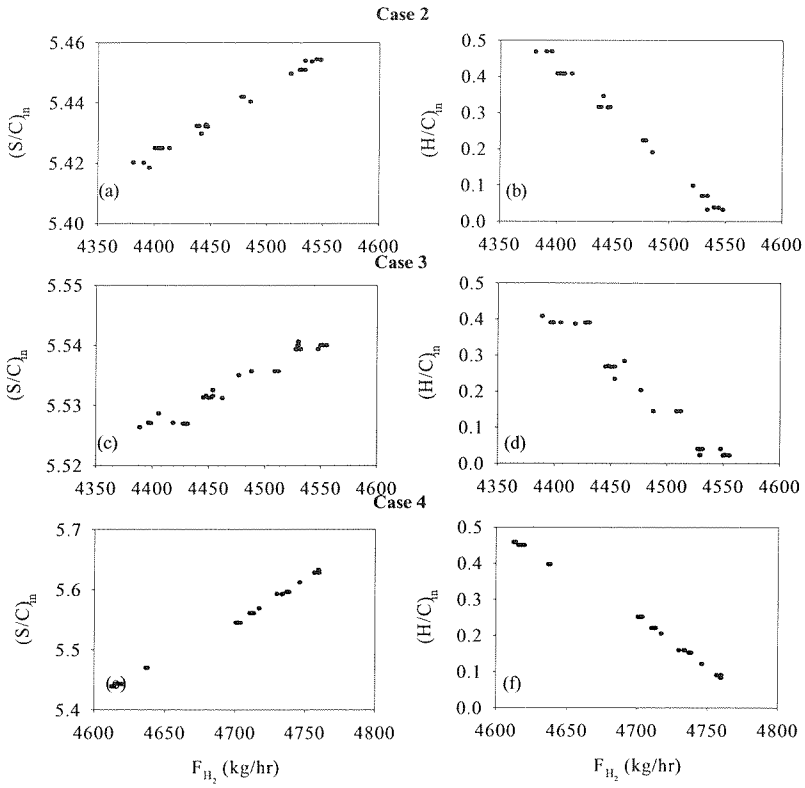

Figure 4. $(S/C)_{in}$ and $(H/C)_{in}$ associated with the Pareto sets of Cases 2 to 4 shown in Fig. 2

optimal $(S/C)_{in}$ indicates that its negligible effect on the objectives (Fig. 4a), while increasing $(H/C)_{in}$ reduces hydrogen production and increases steam generation (Fig. 4b). Optimal values of A to E and z^* remain relatively unchanged, suggesting that the same optimal heat flux profile (shown in Fig. 5) applies to all chromosomes. Similar to Case 1, the heat flux is maximum in the initial sections of the tube before it decreases steadily towards the reformer exit, consistent with the heat demanded by the reactions. However, the heat flux is higher than for Case 1. A higher heat flux indicates that more heat is supplied to the reformer, which for the same extent of reaction in the tubes, raises the outlet temperature. In Case 1, the constraint on Q_{E1} (Eq. (10)) restricts the maximum heat that may be recovered from the reformer effluent and thereby the optimal reformer heat duty that will lead to the best overall performance of the reformer and shift converters. For Case 2, in the absence of this constraint, a higher furnace duty is possible which results in a greater extent of reaction in the reformer. At the same time, more heat can be recovered from the reformer effluent for steam generation.

In Case 1, for a fixed reformer effluent enthalpy, the lowest $T_{HTS,in}$ was limited by the duty of the heat exchanger at the reformer exit (Eq. (10)). Without this constraint in

Case 2, the optimal values for $T_{HTS,in}$ are about 25 K lower than for Case 1 (Table 1). Lower temperatures in the shift converters favour the exothermic shift conversion reaction (Eq. (2)) thus leading to increased hydrogen production. At the same time, more heat of reaction can be recovered in the heat exchanger, E1 for steam generation. However, $T_{HTS,in}$ is not at its lower limit despite the removal of the constraint on Q_{E1} (Eq. (10)). This can be explained by the decrease in the rate of reaction with temperature. Hence, there exists an optimum $T_{HTS,in}$ that balances kinetic and thermodynamic considerations to achieve the maximum extent of reaction in the shift reactor. This is consistent with the observation made by Elnashaie and Alhabdan [14] for adiabatic shift reactors. $T_{LTS,in}$ is also about 2 K lower for Case 2 than for Case 1.

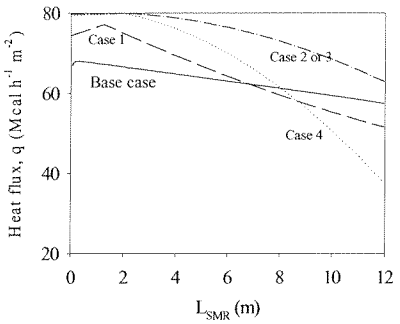

Figure 5. Reformer heat flux profiles representative of the Pareto sets shown in Fig. 2

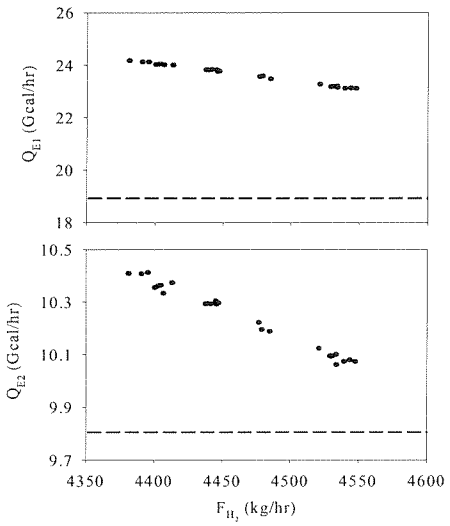

Figure 6. Heat duties of waste-heat exchangers (Q_{E1} and Q_{E2}) associated with the Pareto-optimal set for Case 2 in Fig. 2, shown as points. Dashed lines are the duties according to the design constraints on heat exchangers (Case 1).

The heat exchanger duties required for operation at optimal conditions are shown in Fig. 6 along with the original design constraints placed on the exchanger duties (Eq. (10)). Capacities of E1 and E2 increase by about 25% and 5%respectively from Case 1. In addition, Fig. 6 shows that exchanger duties have opposite effects on hydrogen and steam production. The reason for this can be explained as follows taking into account the constant $T_{SMR,in}$, heat flux profile, $T_{HTS,in}$ and $T_{LTS,in}$ for all chromosomes at the optimum (Table 1 and Fig. 5). Increase in Q_{E1} and Q_{E2} implies that more heat is recovered in the heat exchangers for raising steam from BFW. At the same time, for the same $T_{HTS,in}$, a higher Q_{E1} indicates that more of the heat input to the reformer is recovered in E1 with less being utilized for reforming reactions. This in turn implies lower methane conversion in the reformer and consequently, lower hydrogen production. On the other hand, a higher Q_{E2} for the same $T_{LTS,in}$ indicates a higher extent of shift reaction (Eq. (2)) in the HTS reactor. This is only possible for a fixed $T_{HTS,in}$ when lower methane conversion in the reformer results in the presence of more steam and less hydrogen in the feed to the HTS reactor, thus favouring the forward shift conversion reaction. Since hydrogen production

from the this reaction is incomparable to that from the same extent of the reforming reactions (Eqs. (1) and (3)), overall hydrogen production is decreased. The higher heat flux (Fig. 5) associated with the chromosomes of Case 2 results in the reformer heat duty being about 15% higher than for Case 1 (Table 1).

Case 3: Optimal Design Of Shift Converters

The Pareto-optimal set for this case (Fig. 2 and Table 1) shows that inclusion of shift converter size as additional decision variables in the optimization does not improve hydrogen production and steam generation significantly, compared to Case 2. The effect of decision variables on the objectives is similar to Case 2 (Fig. 4). Typical optimal heat flux profile (Fig. 5) of the chromosomes of the Pareto set in Case 3 and heat duty (Table 1) are indistinguishable from that of Case 2. For all chromosomes, L_{shift} and D_{shift} are at their upper bounds, and the volume of the shift converters doubles compared to Case 2 (Table 1). This may not be economical since the improvement in objectives is marginal.

Case 4. Optimal Design Of Steam Reforming Furnace

The Pareto set for this case (Fig. 2) shows that retrofitting the steam reformer along with other units produces about 5% and 15% improvement respectively in hydrogen and steam production over Case 3. Decision variables associated with two selected chromosomes of Case 4 are listed in Table 1. Effect of decision variables on the objectives is similar to that in the previous cases.

The performance of the reformer is highly dependant on the heat supplied. This is especially true in the initial part of the reformer tube where the bulk of reactions takes place and the extent of reaction is limited by the heat available to maintain high temperatures. Heat supply is dependant on heat transfer area and heat flux. Previous retrofitting cases have all been found to be near or at the upper bound of the allowable heat flux in the initial part of the tube. This constraint can be relaxed at the expense of higher operating severity leading to shortened tube life. Hence, it is better to increase reformer heat duty by increasing tube surface area. The largest surface area would be obtained if both the number and length of tubes are at their upper bounds. While the tube length is at its upper bound, the same is not true of the number of tubes (Table 1). This is attributed to the constraint on the maximum tube wall temperature (Eq. (6)) which limits the allowable temperature rise of the process gas. This in turn constrains the maximum heat duty supplied to the reformer. It is also for this reason that the reformer inlet temperature, $T_{SMR,in}$ is not at its upper bound (Table 1) as in the previous cases.

An optimal heat flux profile representative of all chromosomes of the Pareto-set for Case 4 is shown in Fig. 5. Similar to previous cases, the heat flux is maintained at its upper bound in the initial part of the tubes before declining steadily with tube length. However, as compared to the previous cases, the profile decreases more rapidly in the later sections of the tube to a heat flux of about 40 Mcal h^{-1} m^{-2} compared to the maximum of 80 Mcal h^{-1} m^{-2}. This is due to the constraint on the maximum tube wall temperature (Eq. (6)). The optimal dimensions of the shift converter are near their upper limits (Table 1). The reformer heat duty associated with this design is about 10% higher than that for cases 2 and 3 (Table 1).

Except for Case 1, each of the retrofitting options studied require capital outlay in addition to increased furnace fuel. Since the economics of hydrogen plant design and

operation, taking both capital and operating costs into account, are highly site specific, cost considerations were not included in the present optimization studies. In general, the unit cost of hydrogen in typical industrial plants is made up of about 60% for energy and utilities and 40% for capital costs [213]. Thus it will be prudent to consider the trade-off between the investment cost involved in the various retrofitting options and the additional productivity that results. Specific cost data, if available, can easily be included in multi-objective optimization.

7. Conclusions

Several design and operational changes are considered to improve the capacity of an existing industrial hydrogen plant for both hydrogen and steam production using multi-objective optimization. Improvement is sought by operating the reforming furnace under an optimal heat flux profile, de-bottlenecking waste-heat exchangers and shift converters, and optimizing the reformer design. Multi-objective optimization provides a wide range of optimal solutions, from which a suitable solution can be selected for implementation. The results show that substantial increase in both hydrogen production and steam generation between 5% and 20% is possible. Optimal values of some decisions variables depend on the specific case. Hence, quantitative optimization is necessary. Increased production of hydrogen and steam requires increased reformer heat duty. So, cost of additional fuel for the reformer furnace as well as investment for equipment changes, if any, should be considered when determining the profitability of the retrofitting options.

Acknowledgements

The authors would like to thank Mr. J. K. Rajesh and Mr. B. S. Mohan for providing many invaluable practical insights into hydrogen production.

Nomenclature

$A - E$	Constants in Eq. (11)
F	Total molar feed rate to the unit (kmol/hr)
F_{H_2}	Flow rate of hydrogen from the unit (kg/hr)
F_{stm}	Flow rate of export steam (ton/hr)
$(H/C)_{in}$	Recycle hydrogen to methane molar ratio in the feed
L_{SMR}	Total length of the steam reformer tubes (m)
L_{shift}	Length of shift converter catalyst bed (m)
D_{shift}	Diameter of shift converter catalyst bed (m)
N_{tub}	Total number of reformer tubes
$P_{SMR,in}$	Pressure at the inlet to the steam reformer (kPa)
q	Heat flux at any location on the reformer tubes (Mcal/m^2-h)
Q	Heat duty (Gcal/h)
$(S/C)_{in}$	Steam to methane molar ratio in the feed
T_{in}	Temperature at the inlet to the section (K)
$T_{w,max}$	Temperature of the outer tube wall (K)
y_i	Mole fraction of component i in the bulk gas

z Axial location in the reformer tube (m)
z^* Axial location in the reformer tube where maximum heat flux occurs (m)

Greek symbols

ΔH_r Heat of reaction (kcal/kmol)

Subscripts

E1 Steam generator
E2 Preheater for boiler feed water
HTS High temperature shift converter
LTS Low temperature shift converter
SMR Steam reformer

References

[1] Rajesh, J. K., Gupta, S. K., Rangaiah, G. P., and Ray, A. K. 2001, Chem. Eng. Sci., **56**, 999.
[2] Adris, A. M., Pruden, B. B., Lim, C. J., and Grace, J. R. 1996, Can. J. Chem. Eng., **74**, 177.
[3] Elnashaie, S. S. E. H., and Elshishini, S. S. 1993, Modeling, Simulation and Optimization of Industrial Catalytic Fixed-Bed Reactors, Gordon and Breach, Amsterdam.
[4] Davies, J., and Lihou, D. A. 1971, Chem. Proc. Eng., **52**, 71.
[5] Glacobbe, F. G., Iaquaniello, G., Loiacono, O., and Liguori, G. 1992, Hydrocarbon Process., **71**, 69.
[6] Rajesh, J. K., Gupta, S. K., Rangaiah, G. P., and Ray, A. K. 2000, Ind. Eng. Chem. Res., **39**, 706.
[7] Deb, K. 1995, Optimization for Engineering Design: Algorithms and Examples, Prentice Hall of India, New Delhi.
[8] Edgar, T. F., Himmelblau, D. M., and Lasdon, L. S. 2001, Optimization of Chemical Processes, McGraw Hill, Boston.
[9] Mitra, K., Deb, K., and Gupta, S.K. 1998, J. Appl. Polym. Sci., **69**, 69
[10] Srinivas, N., and Deb, K. 1995, Evolutionary Computation, **2**, 221.
[11] Bhaskar, V., Gupta, S. K., and Ray, A. K. 2000, Rev. Chem. Eng., **16**, 1.
[12] Xu, J., and Froment, G. F. 1989, AIChE J., **35**, 88.
[13] Carey, G. F., and Finlayson, B. A. 1975, Chem. Eng. Sci., **30**, 587.
[14] Elnashaie, S. S. E. H., and Alhabdan, F. M. 1989, Mathematical and Computer Modeling, **12**, 1017.
[15] Singh, C. P. P., and Saraf, D. N. 1979, Ind. Eng. Chem. Process Design and Development, **18**, 1.
[16] Rostrup-Nielsen, J. R. 1984, Catalytic Steam Reforming, A. R. Anderson, and M. Boudart (Eds.), Catalysis – Science and Technology, Vol. 5, Springer, Berlin.
[17] King, D. L., and Bochow, C. E., Jr. 2000, Hydrocarbon Process., **79**, 39.
[18] Ettourney, H. M., Shaban, H. L., and Nayfeh, L. J. 1993, Trans. IChemE, **71A**, 189.
[19] Ahmed, K., Islam, K. A., and Ali, S. 1994, Trans. IChemE, **72A**, 645.
[20] Ridler, D. E., and Twigg, M. V. 1989, Steam Reforming, M. V. Twigg (Ed.), Catalyst Handbook, Wolfe Publishers, London.
[21] Shahani, G. H., Garodz, L. J., Murphy, K. J., Baade, W. F., and Sharma P. 1998, Hydrocarbon Process., **77**, 143.
[22] Goldberg, D. E. 1989, Genetic Algorithms in Search, Optimization, and Machine Learning, Addison-Wesley, Reading, Mass.

Appendix I

Nondominated Sorting Genetic Algorithm (NSGA), developed by Srinivas and Deb [10] to solve multi-objective optimization problems, generates a set of solutions which are non-dominating over each other. Two solutions are said to be nondominating if an improvement in one of the objectives is accompanied by a deterioration in one (or more) of the other objective function(s) when moving from one solution to another. The final set of non- dominating solutions is referred to as a Pareto-optimal set.

A flowchart of NSGA is shown in Figure A1. NSGA differs from the original GA (Deb [7] and Goldberg [22]) in the way the selection operator works. In the former, the randomly generated solutions are sorted into imaginary enclosures called fronts. All the chromosomes within the same front are mutually non-dominating. Each front is assigned a progressively lower common (dummy) value of the fitness function. Then, each chromosome in any front is assigned an individual value of the fitness function which is obtained by dividing the dummy fitness value for the front by the niche count of the individual chromosome. (The niche count is a parameter proportional to the number of chromosomes in the neighborhood of this chromosome within the same front.) This action spreads chromosomes and also maintains the diversity of the gene pool. All other operations performed are similar to those in the traditional GA.

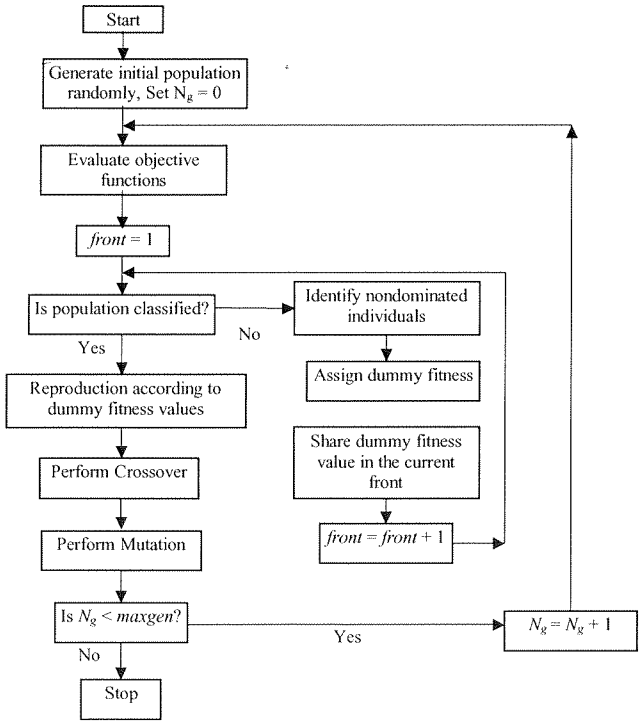

Figure A1 A flowchart of NSGA (adapted from Mitra et al. [9])